Chapter 5

The Effect of Yttria on the Properties of Olivine

Suleyman Serdar Pazarlioglu[1]

Ebru Sumen[2]

Hasan Gokce[3]

Abstract

Due to the increasing trend in the use of olivine, in this study, mixtures were prepared by adding Y_2O_3 at the rates of 1, 2.5, 5, 10 and 20 percent by weight to olivine obtained from a facility and these mixtures were gradually sintered at temperatures of 1100, 1200, 1300, 1400, 1450 and 1500 °C for 3 hours. The findings showed that Y_2O_3 additives improved the mechanical properties of olivine. The effect of the interphase observed in the microstructure of composite structures increased the strength by reducing the glassy phase and caused grain thinning. The best results in each group studied were achieved at the sintering temperature of 1400ºC, and it was observed that these values decreased at temperatures above this. It was observed that the reason for this decrease was due to increasing average grain size and crack formation in the microstructure.

Introduction

Olivine group minerals that crystallize in the orthorhombic system mainly consist of Mg^{2+} and Fe^{2+} silicates and are in the ortho-silicate group [1]. Developed countries have started to ban the use of minerals and raw materials containing free silica through the laws they have enacted in order to prevent risks that may arise in terms of occupational and environmental health [2]. Another important reason why the use of olivine increases from year to year is that dunites found in masses are suitable for open mining. Additionally, they are obtained directly as by-products during the enrichment

1 Dr. Öğr. Üyesi, Marmara University, spazarlioglu@marmara.edu.tr
ORCID ID: 0000-0002-7870-8418

2 Student, Marmara University, ebrusumen2@gmail.com ORCID ID: 0000-0001-9575-3627

3 Dr, Istanbul Technical University, gokceh@itu.edu.tr ORCID ID: 0000-0001-7892-5642

https://doi.org/10.58830/ozgur.pub251.c1222

of chrome ore. These features can provide significant reductions in operating and production costs. Türkiye has rich reserves of olivine. However, it is one of the minerals that we cannot adequately utilize in production or use due to reasons such as lack of studies, lack of investment or lack of market [3]. In addition to its resistance to thermal shocks and easy shaping, its reusability rate is higher than silica. Olivine is widely used as refractory mortar sand in all sectors requiring high temperature insulation and resistance [4]. The initial sintering temperature of olivine with high forsterite content is 1450°C and its high melting temperature, resistance to thermal shock and slag corrosion make olivine a refractory material. Olivine is used especially in the production of fire-resistant forsterite bricks and in the lining of concrete in high-temperature furnaces. Fire-resistant forsterite bricks are preferred for lining the inner walls of cement kilns and metallurgical furnaces with high heat treatments. Olivine, which can keep harmful gas formation at a low level, is also used in hospital waste and toxic substance disposal and in the burner lining of silos [5]. In a study by Furlani and Maschio, olivine sand was tested for tile production. Olivine sand and kaolin clay were used in certain proportions and sintered at temperatures such as 1250°C and many properties such as hardness, toughness, bending strength, water absorption and deformation were examined. They stated that 60% olivine sand and 40% kaolin content provided optimum properties, but the produced product could be used as industrial tiles [6]. In their study, Çolak et al. evaluated the addition of 10, 20, 30 and 40% MgO by weight to investigate the suitability of Ağla-Köyceğiz dunites for olivine brick production, but as a result of their study, they stated that MgO-added olivine could be used as industrial tiles [7]. Furlani et al. studied the sintering behavior of olivine or olivine/alumina powder mixtures. For this purpose, the powders were ground, uniaxially pressed into samples, and sintered at temperatures ranging from 1100 to 1300 °C. The obtained samples were characterized by water absorption, shrinkage, phase composition and density. They stated that compositions containing 5%, 10% and 20% Al_2O_3 had a sintering behavior similar to that of pure olivine and low residual porosity occurred when fired at 1300°C [8]. İlker Acar examined an olivine sample obtained as final residue from the chromite enrichment plant in terms of its sintering properties and potential for use as a refractory raw material. For this purpose, the cylindrical samples were prepared and then sintered in the laboratory oven at temperatures of 1300, 1400, 1450 and 1500°C for 2 hours. The refractoriness property was evaluated with some physical and mechanical tests such as density, water absorption, porosity, firing shrinkage and compressive strength after sintering. Additionally, phase developments and microstructural changes due to sintering were determined in detail by X-ray diffraction (XRD) and scanning electron microscopy (SEM) analyses, respectively. According to experimental results, density and firing shrinkage values increased with increasing temperature, while porosity and water absorption values decreased. Specifically, the bulk density and shrinkage values ranged from 2.33 to 2.60 g/cm^3 and 1-5%, respectively. Porosity values of 24.10% and 15.68% were obtained after sintering at 1300 and 1500 °C, respectively. After sintering between 1300 and 1450 °C, the compressive strengths gradually increased from 46.90 to 55.86 MPa. Then, a sudden increase to 93.44 MPa was observed. Accordingly, thermo-optical analysis showed that olivine exhibited a sintering point of 1478°C and no softening until 1500°C. However, the formation of enstatite with a low melting temperature was detected by XRD and SEM analysis, which also indicated the crystallization of forsterite and spinels with increasing amorphous phase and increasing temperature. The overall results showed that the olivine sample used had a promising potential as a refractory raw material, mainly due to its high MgO content, low loss on ignition (LOI) value and suitable particle size [9]. In his study, Nuri A. aimed to examine the usability of olivine powder as a plasma coating powder to work against wear and to examine its microstructure and properties after coating. For this purpose, olivine mineral was coated on the steel surface to improve the working performance of 316L stainless steel, which is widely used in industry [10]. Furlani et al. investigated the sintering performance of a series of samples containing olivine and cerium oxide powder in the range of 3-40% by weight, and they stated that samples containing 40% by weight cerium oxide shrank at lower temperatures than the others [11]. Emre S. and others investigated the corrosion protection effectiveness of the reinforced concrete reinforcement embedded in the concrete produced by using olivine waste in concrete. In order to investigate this effect, C30 class concrete, which is widely used, was chosen as the target compressive strength. Concrete samples were produced using olivine waste (OW) ground to cement fineness to be compared with reference concrete. Olivine waste (OW) was replaced with cement in concrete at the rates of 5%, 10%, 20% and 40% by volume, and 150x150x150 mm cube samples were produced and subjected to normal water curing at 21±1ºC for 7 and 28 days. At the end of the curing process, density and compressive strength tests were applied to OW concrete samples. There has been a certain decrease in the density and compressive strength values of hardened concrete. However, samples containing 5%, 10% and 20% waste reached strength above the target compressive strength [12]. Dobrzhinetskaya et al. investigated the solubility of titanium oxide in olivine, but did not examine its microstructural and mechanical effects on olivine [13]. As a result, the following conclusion was reached in the studies on olivine in the literature:

- The effects of alumina, magnesium oxide, cerium oxide, basalt and kaolin additions on the microstructural properties of olivine were studied, and the sintering temperature of olivine, which has a sintering temperature of 1478^oC due to sintering processes carried out between 1000-1300^oC.
- It is used industrially as sand and/or lining material in electric arc furnaces and as industrial tiles.

However, the properties of refractory bricks used in the ceiling, wall and floor of electric arc furnaces used in the production of products from scrap in the iron and steel industry are as can be seen in Table 1-3 [14].

Table 1 Types and properties of refractory bricks used in the ceiling of electric arc furnaces

Property	High Alumina Bricks			Simple brick	High alumina precast		
	A	B	C	D	E	F	G
Apparent density	3.40	3.62	3.66	3.47	3.14	3.09	3.65
Bulk density (g.cm^{-3})	2.73	3.02	3.18	3.05	2.77	2.69	3.15
Apparent porosity (%)	19.9	16.8	13.1	12.1	14.0	12.9	13.7
Cold crushing strength (kg.cm^{-2})	340	770	780	870	340	400	500
Refractoriness (SK)	≥37	≥37	≥38	-	≥37	≥38	≥38

Table 2 Types and properties of refractory bricks used in the walls of electric arc furnaces

Property	MgO-C brick				$MgO-Cr_2O_3$	
	K	L	M	N	O	P
Apparent density	3.06	3.09	2.65	2.81	3.75	3.78
Bulk density (g.cm^{-3})	2.98	2.99	2.83	2.72	3.25	3.27
Apparent porosity (%)	2.5	3.3	3.9	3.2	13.4	13.4
Cold crushing strength (kg. cm^{-2})	448	507	352	270	883	953

Table 3 Specifications of the wall refractor around the EBT(Z) tap hole

Property	MgO	Al_2O_3-SiC-C	MgO	$MgO-Cr_2O_3$
	Pipe	Terminal	Arm	Bottom and round pipe
Apparent density	2.85	2.98	3.00	> 2.85
Cold crushing strength (kg.cm^{-2})	390	600	872	> 400

Ytrrium oxide (Y_2O_3) is a highly refractory material with a fusion point of about 2400-2680°C. It is quite well sintered to a high density, and the ceramics based on it have excellent strength and dielectric properties, and a relatively low coefficient of thermal expansion [15]. Because of its superior inertness to chemical attack from molten Ti alloys during investment casting, yttria has been widely used as a face-coat material in the investment casting of titanium aluminide alloys for a number of years [16]. It helps to increase the sinterability of Al_2O_3 [17], tungsten [18], ZrO_2 [19] and etc.

Due to the increasing trend in the use of olivine, in this study, mixtures were prepared by adding Y_2O_3 at rates of 1, 2.5, 5, 10 and 20 by weight% to olivine, and these mixtures were gradually mixed and then sintered for 3 hours at temperatures of 1100, 1200, 1300, 1400, 1450 and 1500 °C. Additionally, olivine without Y_2O_3 was sintered at these temperatures to provide comparison.

Experimental Procedure

The olivine used in the current study was supplied from Beykrom Madencilik A.Ş. Y_2O_3 in spherical form and with an average grain size of 5 μ, purchased from Nanografi Nano Technology company, were used as reinforcement material. It was added to olivine at the rate of 1, 2.5, 5, 10 and 20% by weight. In the first stage of the experimental stage, mixtures were prepared in the mentioned proportions by weight on a precision balance, and these mixtures were ground and homogenized in a Retsch PM100 model ball mill device at 180 rpm for 2 hours. Ethyl alcohol (C_2H_5OH) used in this process; CAS number: 64-17-5, density is 0.805 - 0.812 g/cm^3 at 20 °C and purity is 96%. In each mixture, 7 samples for 6 different temperatures (1100, 1200, 1300, 1400, 1450 and 1500°C) were obtained by pressing method. A mixture of 30 ml of ethyl alcohol and approximately 1.5 grams of zinc stearate ($Zn(C_{18}H_{35}O_2)_2$) was used as mold lubricant during the sample pressing process. The samples were pressed at 3 tons in a Compac Hydraulic A/S brand 6-ton capacity hand-held hydraulic press, with a sample length of 10.8-11.2 mm in order to prevent lamination between olivine powders. In the pressing process, a mold made of 2347 quality heat-treated steel with a hardness over HRC 50 and with dimensions of 60 mm height, 60 mm outer diameter and 11 mm inner diameter was used. Before sintering, the samples were subjected to moisture removal and the furnace temperature increase rate (ramp) was set as 5°C/minute in order to prevent the formation of residual and thermal stress fields from causing cracks in micro and macro dimensions. The symbol Y was used for Y_2O_3 in defining the mixtures, and pure olivine, apart from olivine- Y_2O_3 mixtures, was also sintered at these temperatures for comparison. 36 different working groups are defined in **Table 4**.

Table 4 Working groups created in the current study with composition and sintering temperature

Working Groups (Composition-Sintering Temperature)					
Olivine-1100°C	Olivine+1Y-1100°C	Olivine+2.5Y-1100°C	Olivine+5Y-1100°C	Olivine+10Y-1100°C	Olivine+20Y-1100°C
Olivine-1200°C	Olivine+1Y-1200°C	Olivine+2.5Y-1200°C	Olivine+5Y-1200°C	Olivine+10Y-1200°C	Olivine+20Y-1200°C
Olivine-1300°C	Olivine+1Y-1300°C	Olivine+2.5Y-1300°C	Olivine+5Y-1300°C	Olivine+10Y-1300°C	Olivine+20Y-1300°C
Olivine-1400°C	Olivine+1Y-1400°C	Olivine+2.5Y-1400°C	Olivine+5Y-1400°C	Olivine+10Y-1400°C	Olivine+20Y-1400°C
Olivine-1450°C	Olivine+1Y-1450°C	Olivine+2.5Y-1450°C	Olivine+5Y-1450°C	Olivine+10Y-1450°C	Olivine+20Y-1450°C
Olivine-1500°C	Olivine+1Y-1500°C	Olivine+2.5Y-1500°C	Olivine+5Y-1500°C	Olivine+10Y-1500°C	Olivine+20Y-1500°C

In order to determine the mechanical properties, samples selected from 7 samples were determined and separated to be used in density, compressive strength and hardness tests for each mixture. The Archimedes method was used in the density test, and the formula stated below and a Precisa brand XB 320M model precision scale with an accuracy of 0.001 g constituted the basic functions of this test.

$$d = \frac{Mk}{Ma-Ms} \quad (1)$$

Here; d: Density (g/cm³), Mk: Dry weight (g), Ma: Suspended weight (g), Ms: Weight in water (g)

In the compression test, Devotrans brand DVT FU 50KN YBS model device was used and after the test, the broken and fragmented samples were beaten in a ceramic mortar until they were powdered suitable for XRD analysis. Additionally, no pre-load was applied during the test and the test speed was 2 mm/min. Hardness measurement was made with a Future-Tech brand and FM-310e model micro hardness tester. During the test, a load of 200 grams was applied for 10 seconds and the average of the hardness results taken from 5 different points. PANalytical X'Pert Pro brand XRD device was used for phase identification. The device allows phase identification from powder diffraction data and uses a ceramic insulated tube (3kW) as the x-ray source and Cu Kα (1.5405 Å) as the wavelength. The percentages of the phases formed as a result of XRD analysis were determined by Rietvield analysis. Finally, a ZEISS EVO-MA10 brand high-resolution scanning electron microscope (SEM) was used for internal structure analysis.

Results and Discussion

Figure 1 shows the mechanical properties of olivine with and without Y_2O_3 additives. In the comparison of pure olivine and olivine-yttrium oxide group, the highest compressive strength value, with an increase of 106% and a value of 197.14±7.505 MPa, was seen in the composition with 20wt% Y_2O_3 at the sintering temperature of 1400°C. Except for the composite structure containing 1wt% Y_2O_3, all mixtures exhibited a similar structure, reaching the highest compressive strength value at 1400°C. Except for the 1wt%Y_2O_3 contributing, in general, as the Y_2O_3 ratio increases, an increasing compressive strength is observed compared to pure olivine, starting from 1300°C. In addition, it is seen that Y_2O_3 additives do not cause a positive effect on the compressive strength values of olivine at sintering temperatures of 1100 and 1200°C, and even reduce its strength in some compositions. The highest hardness value was observed with a 31% increase and a hardness value of 629.38±7.04HV at the sintering temperature of 1400°C, but only in the composition with 20wt%Y_2O_3 added. Additionally, from this graph, it can be mentioned that there is a continuous increase in hardness values as the Y_2O_3 ratio increases. From the hardness chart evaluations, it can be interpreted that, just like the compressive strength, additives do not have a positive effect on the hardness values of pure olivine at sintering temperatures of 1100 and 1200°C. When all evaluations are taken into consideration, it is seen that the compressive strength and hardness graphs give approximately similar results. In the olivine-Y_2O_3 graph, an increase of 18% compared to pure olivine and the highest density with a density value of 3.359±0.008g/cm^3 was seen in the 20% Y_2O_3-doped composite structure sintered at 1450°C. In addition, the highest density in 1wt%, 2.5wt% and 10wt% Y_2O_3 is seen at 1400°C, while there is a significant decrease in the 20wt% Y_2O_3 added structure sintered at 1500°C. The highest density (2.845±0.014 g/cm^3), hardness (479.44±8.220 HV) and compressive strength (95.52±6.36 MPa) for pure olivine were obtained at 1400°C, and these values decreased with increasing temperature and they were calculated as 2.786±0.012 g/cm^3, 369.78±5.370 HV and 45.18±4.04 MPa, respectively. The addition of Y_2O_3 at amount of 20wt% contributed to an increase of 18%, 31% and 106% in the density, hardness and compressive strength values of olivine, respectively. The reason for this is due to the intermediate phases formed (Figure 3) and the decrease in average grain size (Figure 4 and 5). The smallest grain size, with a value of 15.759±2.484, was observed in the structure with 20% Y_2O_3 addition at the sintering temperature of 1400ºC. The density and mechanical property data appear to be consistent with the composition and temperature at which grain size gives its smallest value. The phase naming and percentages at the composition and temperature of 20wt% Y_2O_3-1400ºC, where the best compressive strength and hardness values are achieved, are as follows: Forsterite: %73.9, Enstatite ($Fe_{0.498}Mg_{1.502}Si_2O_6$): %14.4 Y_2SiO_5: %1.2, Fe_2YO_4: %1.7 $Fe_{2.454}Si_{0.546}O_4$: %1.4 , Fe_2SiO_4 : %2.3 , Y_2O_3 : %2.2, β-$Y_2Si_2O_7$: % 2.9. It is seen that the resulting interphase percentages reach their highest values in olivine composite structures with 20% Y_2O_3 added. These structure formations prevented grain growth and caused an increase in the strength of olivine.

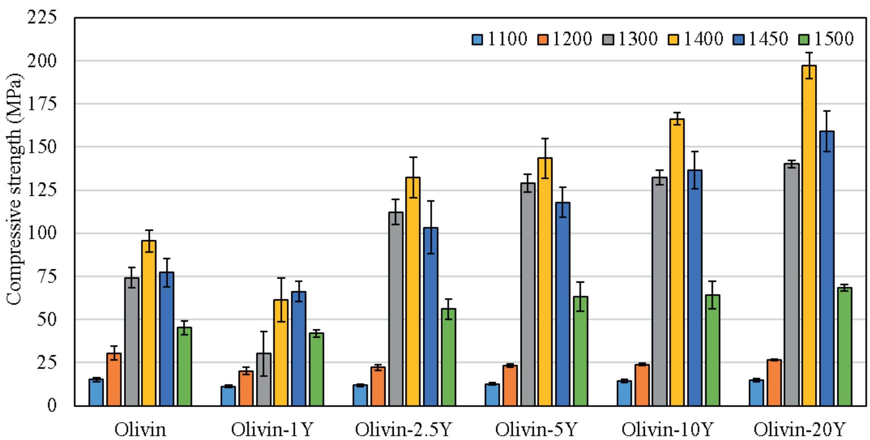

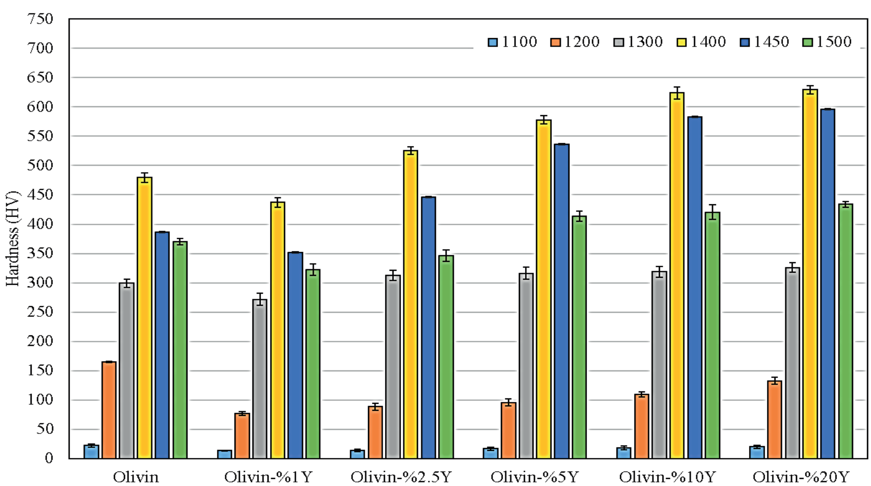

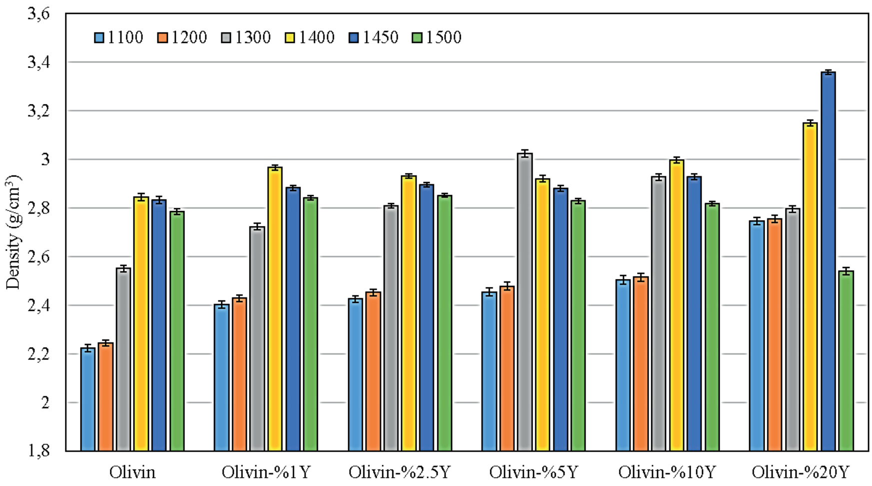

Figure 1 The mechanical properties of olivine with and without Υ_2O_3 additives

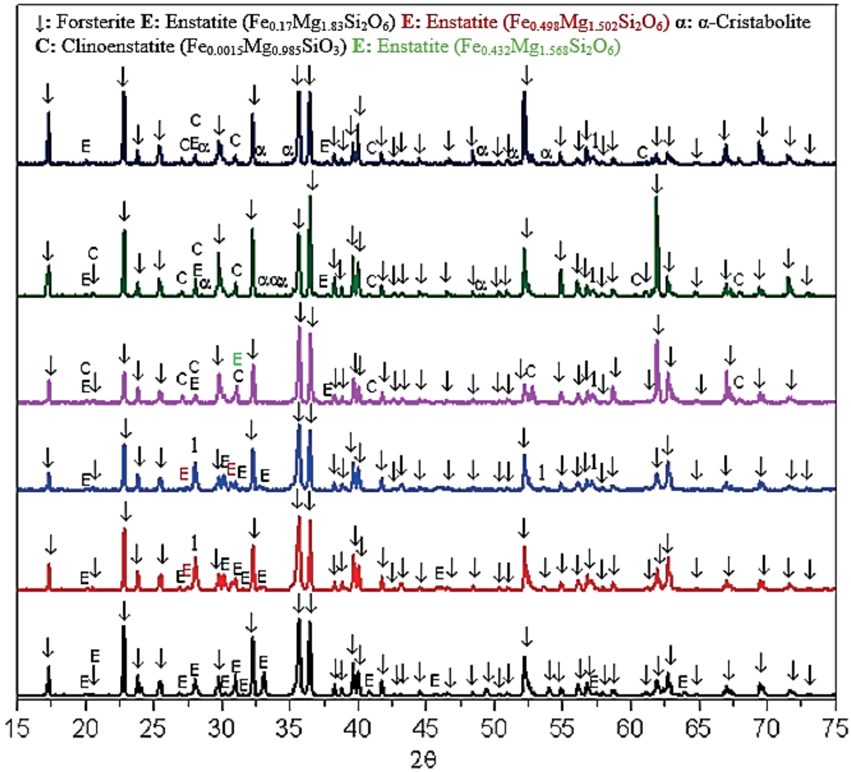

Figure 2 XRD analysis of pure olivine

Table 4 Chemical composition and percentages of the phases formed by pure olivine at the 6 sintering temperatures subject to the experiment

Temperature (°C)	Chemical composition (%)
1100	↓: Forsterite: %72.4, E: Enstatite ($Fe_{0.17}Mg_{1.83}Si_2O_6$): %27.6
1200	↓: Forsterite: %61.7, E: Enstatite ($Fe_{0.17}Mg_{1.83}Si_2O_6$): %37.8, Enstatite ($Fe_{0.498}Mg_{1.502}Si_2O_6$): %0.5
1300	↓: Forsterite: %63.6, E: Enstatite ($Fe_{0.17}Mg_{1.83}Si_2O_6$): %36.2, Enstatite ($Fe_{0.498}Mg_{1.502}Si_2O_6$) : %0.2
1400	↓: Forsterite: %67.5, E: Enstatite ($Fe_{0.17}Mg_{1.83}Si_2O_6$): %4.0, C: Clinoenstatite ($Fe_{0.0015}Mg_{0.985}SiO_3$): %27.4 , E: Enstatite ($Fe_{0.432}Mg_{1.568}Si_2O_6$): %1.1
1450	↓: Forsterite: %79.0, E: Enstatite ($Fe_{0.17}Mg_{1.83}Si_2O_6$): %1.9, C: Clinoenstatite ($Fe_{0.0015}Mg_{0.985}SiO_3$) : %18.2, α: α-Cristobalite (SiO_2): 0.9
1500	↓: Forsterite: %76.6, E: Enstatite ($Fe_{0.17}Mg_{1.83}Si_2O_6$): %1.5, C: Clinoenstatite ($Fe_{0.0015}Mg_{0.985}SiO_3$) : %20.5, α: α-Cristobalite (SiO_2): 1.4

Figure 2 and **Table 4** show the XRD analysis of pure olivine and chemical composition and percentages of the phases formed by pure olivine at the 6 sintering temperatures subject to the experiment, respectively. Pure olivine contains forsterite, enstatite, clinoenstatite, and α-cristabolite phases. The structure of olivine, formulated as Mg_2SiO_4, consists of isolated SiO_4 tetrahedra in which each of the oxygen atoms of the tetrahedra is shared by three octahedral cations. Magnesium orthosilicate, whose chemical formula is Mg_2SiO_4 and whose chemical name is Forsterite, has a variety of applications due to its high thermal expansion coefficient close to that of zirconia and many superior properties [20]. The enstatite phase, which is the other most important phase observed in the study after forsterite, is a pyroxene mineral, as will be stated. Pyroxenes are commonly found in volcanic rocks because they are anhydrous silicates and are unstable in the presence of water. Pyroxenes are classified as inosilicates because their structure is based on the interlocking of silicon chains surrounded by four oxygen atoms. Orthoenstatite is an important component of basic and intermediate grade igneous rocks, usually associated with augite, olivine and plagioclase. Protoenstatite transforms to orthoenstatite in the absence of shear stress and requires slow cooling rates; this is indicative of a reconstructive phase transition. Under shear stress, protoenstatite transforms into lower clinoenstatite, and this transformation is much faster. Instead, a direct phase

transition between ortho- and lower-clinoenstatite is not observed. High clinoenstatite at high temperature and high pressure gradually turns into orthoenstatite [21]. Cristobalite is a common silica polymorph in ceramics because it can crystallize in SiO_2-rich systems during high-temperature processes. Cristobalite is stable at high temperatures and low pressures, and upon cooling it spontaneously transitions into the displacement phase towards tetragonal α-cristobalite. The transition is accompanied by a 5% decrease in volume, causing the crystals to crack on cooling. The resulting fish-scale texture is indicative of cristobalite undergoing a displacement transition [22]. **Figure 3** shows the XRD analysis of Y_2O_3 added samples. The $FeSiO_3$ phase, which forms in a composite structure with only 1% Y_2O_3 added at all sintering temperatures starting from 1300 °C, is a synthetic high-pressure phase called ferrosilite and does not exist in nature. Just as forsterite and fayalite are defined as two solid solution intervals in olivine, enstatite and ferrosilite form a solid solution interval as extremes [21]. The percentage of the ferrosilite phase increases as the temperature increases in this composition, and it is involved in the formation of magnesioferrite ($Fe_{2.454}Si_{0.546}O_4$) and fayalite (Fe_2SiO_4) phases, which have a spinel structure and are formed for the first time in a 2.5% Y_2O_3-doped composite structure. The percentage of this two-phase structure increases with temperature. While the phases at 2.5% are nominally preserved in 5% Y_2O_3-doped structures, the Y_2O_3 phase was formed in the structure starting from the 1300 °C sintering temperature of the 10% Y_2O_3-doped composite structure and continued its existence until 20% Y_2O_3- 1500 °C. The β-Y_2Si_2O7 phase first formed at 10% Y_2O_3-1450°C. When the mechanical properties and phase structures of Y_2O_3-Olivine composite structures were examined, it was seen that as the Y_2O_3 reinforcement increased, the strength increased due to the proportional increase in Fe-rich oxide structures such as Fe_2YO_4, $Fe_{2.454}Si_{0.546}O_4$ and Fe_2SiO_4. It is thought that high density enstatite and β-$Y_2Si_2O_7$ phase are effective in reaching the highest density at 1450°C with the addition of 20% Y_2O_3. Additionally, the Y_2O_3 phase also provided an increase in density with a density of 5.1 g/cm³ [23]. It is seen that the resulting interphase percentages reach their highest values in olivine composite structures with 20% Y_2O_3 added. These structure formations prevented grain growth and caused an increase in the strength of olivine. The Y_2SiO_5 phase formed at all Y_2O_3 doping ratios has a low elastic modulus, low oxygen permeability and a relatively high coefficient of linear thermal expansion ($(8.36 \pm 0.5) \times 10^{-6}$ K^{-1}) [24].

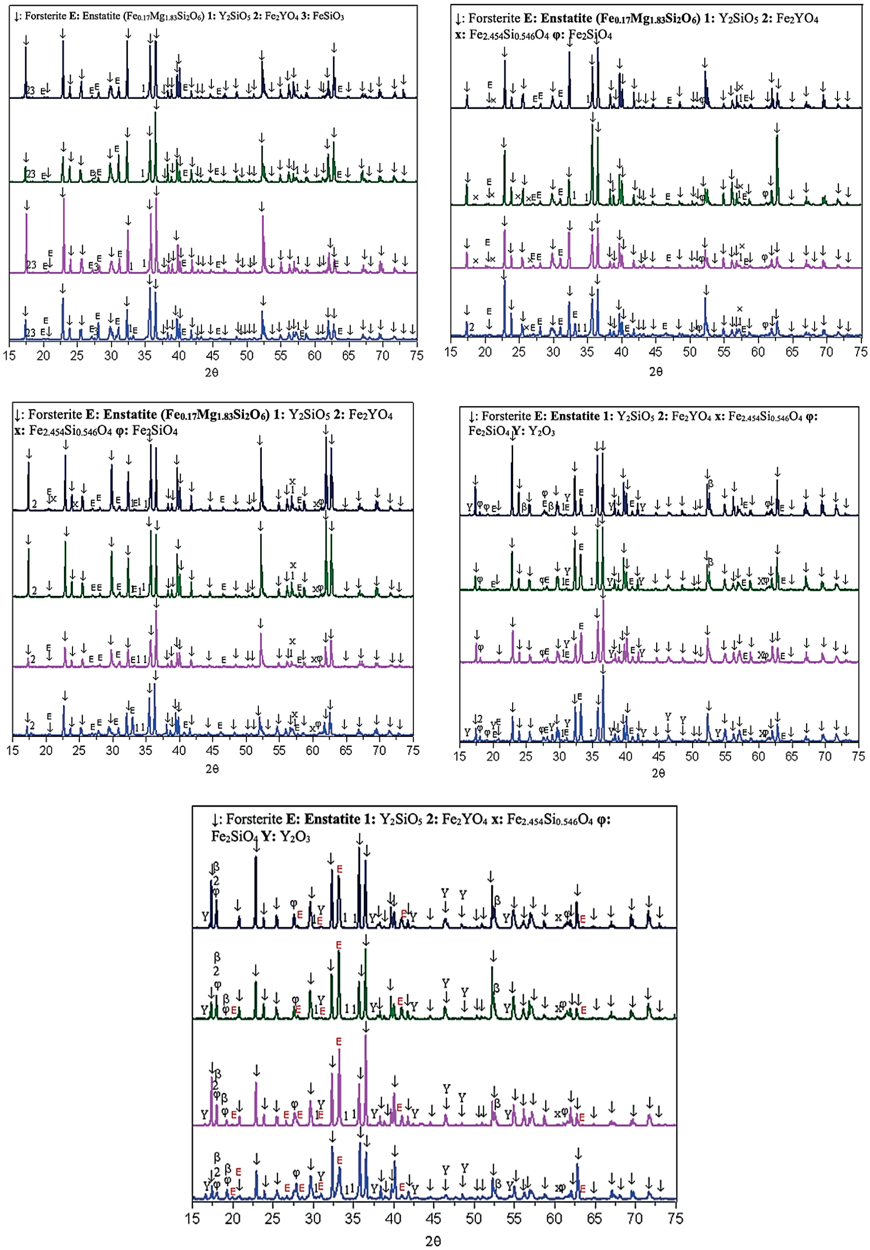

Figure 3 XRD analysis of Y_2O_3 added samples.

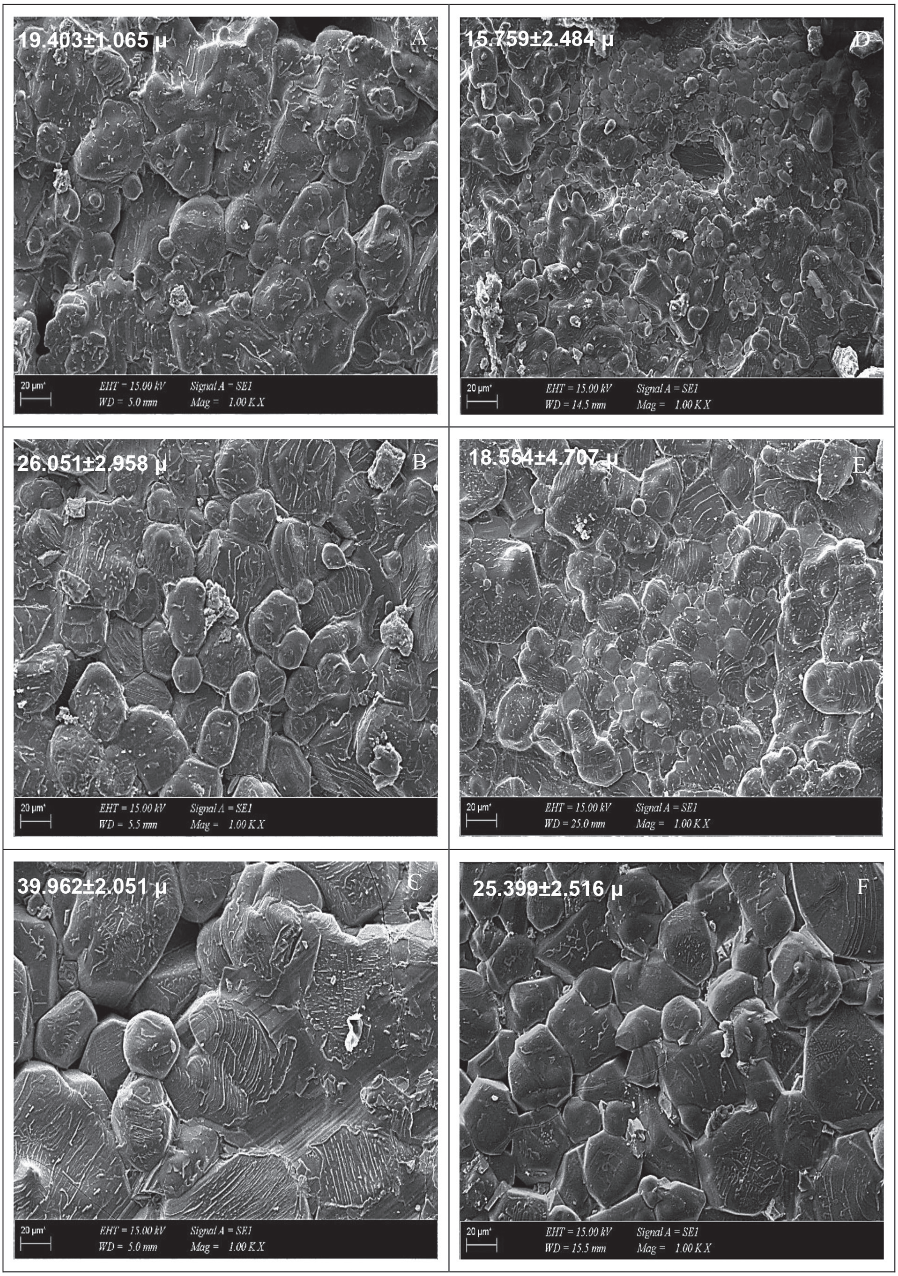

Figure 4 SEM images and average grain size values of pure olivine at (a) 1400, (b) 1450 and (c) 1500°C and Olivine-20Y at (d) 1400, (e) 1450 and (f) 1500°C temperatures

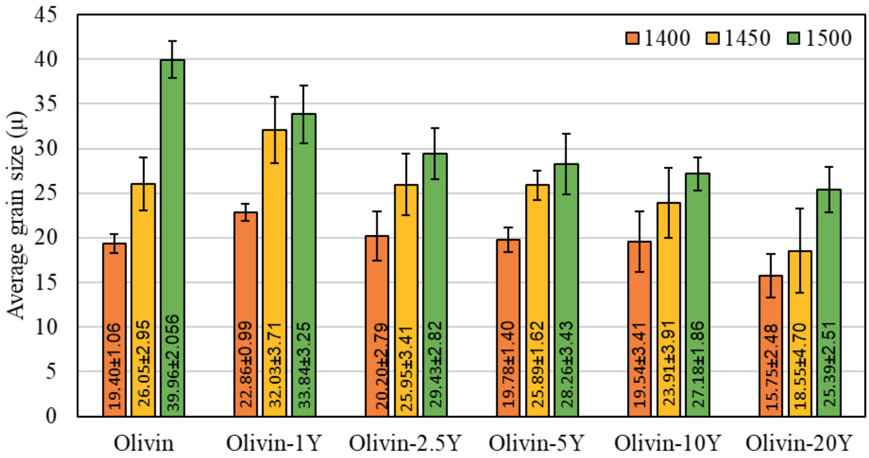

Conclusion

In this study, the effects of adding ytrria to olivine at 1, 2.5, 5, 10 and 20 weight ratios were examined. The best mechanical properties were achieved with the addition of 20% yttria to olivine and a temperature of 1400^{o}C.

Acknowledgement

The authors would like to thank Marmara University BAPKO unit for providing support within the scope of the project no: FYL-2023-10867.

References

[1] Maden Tetkik ve Arama Genel Müdürlüğü, Olivin, http://www.mta.gov.tr/v3.0/bilgi-merkezi/olivin (Erişim Tarihi:10.05.2022)

[2] Erkrom Madencilik, Olivin, http://erkrommaden.com.tr/olivin.html (Erişim Tarihi:10.05.2022)

[3] Devlet Planlama Teşkilatı, 2007, Dokuzuncu Beş Yıllık Kalkınma Planı, Madencilik ÖİK Raporu (No:690,

[4] ORE-MET Olivine Sands, Refractory Mixes, http://www.oremet.net/content/mining (Erişim Tarihi:11.05.2022)

[5] Örgün, Y., 2012, 21. Yüzyılda Olivin ve Türkiye'nin Olivin Potansiyeli, Madencilik ve Türkiye Dergisi, 23:62-74.

[6] Furlani, E. and Maschio, S. Mechanical properties and microstructure of fast fired tiles made with blends of kaolin and olivine powders, Ceramics International, 39, (2013), 9391-9396.

[7] Çolak, M. Refractory Olivine Bricks Application from the Ağla-Köyceğiz (Turkey) Dunite. Key Engineering Materials, 264-268, (2004), 1799-1802.

[8] Furlani, E., Aneggi, E., Maschio, S. Sintering Behaviour of Waste Olivine and Olivine/Alumina Blends. Materials, 7, 2014, 4773-4788.

[9] Acar, I. Sintering properties of olivine and its utilization potential as a refractory raw material: Mineralogical and microstructural investigations. Ceramics International, 46, (2020), 28025-28034.

[10] Aydınlı, N. Plazma Sprey Kaplamada Olivinin Değerlendirilmesi ve Kaplama Özelliklerinin İncelenmesi, Yüksek lisans tezi, Sakarya Üniversitesi, 2008.

[11] E. Furlani, E. Aneggi, C. de Leitenburg, A. Trovarelli, S. Maschio, Sintering behaviour of olivine–ceria blends, Ceramics International, 41[5], (2015), 6293-6298.

12] Sancak, E., Çoban, Ö. Olivin Atıklarının Betonda Kullanımının Betonarme Donatısının Korozyon Özelliklerine Etkisi. Selçuk Üniversitesi Mühendislik, Bilim ve Teknoloji Dergisi, 2, (2014), 26-41.

[13] Dobrzhinetskaya, L., Bozhilov, K.N., Green, H.W. The solubility of TiO in olivine: implications for the mantle 2 wedge environment. Chemical Geology, 163, (2000), 325-338.

[14] Ghosh, B.N. Refractories for electric arc furnace, chrome-extension://efaidnbmnnnibpcajpcglclefindmkaj/https://eprints.nmlindia.org/2822/1/37-51.PDF (Erişim Tarihi:11.11.2022)

[15] Borovkova, L.B., Lukin, E.S., Poluboyarinov, D.N., Sapozhnikova. E. B. Sintering and properties of yttrium oxide ceramics. Refractories, 11, (1970), 717-722.

[16] Cheng, X., Yuan, C., Green, N.R., Withey, P.A. Sintering mechanisms of Yttria with different additives. Ceramics International, 39[5], (2013), 4791-4799.

[17] Zhao, Z., Yang, Z., Yu, Z., Fan, M., Bai, J., Yu, J., Ren, Z. Influence of yttrium oxide addition and sintering temperature on properties of alumina-based ceramic cores. International Journal of Applied Ceramic Technology, 17[2], (2020), 685-694.

[18] Youngmoo, K., Moon-Hee H., Sung-Ho, L., Eun-Pyo, K., Seong, L., Joon-Woong, N. The effect of yttrium oxide on the sintering behavior and hardness of tungsten. Metals and Materials, 12[3], (2006), 245-248.

[19] Flegler, A.J., Burye, T.E., Yang, Q., Nicholas, J.D. Cubic yttria stabilized zirconia sintering additive impacts: A comparative study. Ceramics International, 40[10], (2014), 16323-16335.

[20] Michel, R., Ammar, M.R., Poirier, J., Simon, P. Phase Transformation Characterization of Olivine Subjected to High Temperature in Air. Ceramics International, 39[5], (2013), 5287-5294.

[21] Nespolo, M. Pyroxenes. Reference Module in Earth Systems and Environmental Sciences. (2020). doi:10.1016/b978-0-12-409548-9.12409-1

[22] Pagliari, L., Dapiaggi, M., Pavese, A., Francescon, F. A Kinetic Study of the Quartz–Cristobalite Phase Transition. Journal of the European Ceramic Society, 33[15-16], (2013). 3403-3410

[23] https://nanografi.com/nanoparticles/yttrium-oxide-y2o3-nanopowder-nanoparticles-purity-99-999-size-25-50-nm/, 05 Ekim 2023.

[24] Sun, Z., Li, M., Zhou, Y. Thermal Properties of Single-Phase Y_2SiO_5. Journal of the European Ceramic Society, 29[4], (2009), 551–557.